 Transactions on Modelling and Simulation vol 10, © 1995 WIT Press, www.witpress.com, ISSN 1743-355X

Boundary element solutions to wave scattering by surface irregularities on a fluid-solid interface

S. Shenoy, T.J. Rudolphi, F.J. Rizzo
Department of Aerospace Engineering and Engineering Mechanics, Iowa State University, Ames, IA 50011, USA

Abstract

The boundary element method is used to solve fluid-solid half-space problems with fluid-filled dimples and air bubbles on the solid surface. The problems, formulated in the Fourier (frequency) domain, are described by the fullspace three-dimensional acoustic and elastodynamic boundary integral equations (BIE), with pressure and displacement serving as primary variables. The techniques developed are general and may be with any kind of incident wave, however, plane waves are used in all numerical experiments. The equations governing the acoustic region are first converted mathematically to equations like those of an elastic region. The two regions are coupled and solved for the displacements using the interface conditions. On obtaining the displacements, the tractions, pressures and pressure gradients are computed using the same interface conditions. The numerical results obtained are verified using reciprocity relations and by comparison with solutions available for the half-space elastodynamic problem.

Introduction

The specialization of the boundary element method for modeling the reflection, transmission, and scattering of an ultrasonic wave, through an infinite fluid-solid interface in the presence of surface dimples, is presented. The method developed here may be used for any type of wave – plane, Rayleigh, etc. It can also be extended (using hyper-singular elements) to deal with surface breaking cracks. The work is motivated by the needs of ultrasonic testers to characterize surface breaking flaws using immersion testing.

Previous work in this area has been restricted to either special surfaces (flat) or special waves (Gaussian). These include: Luco and Apsel[1] for a layered

half-space, Rizzo *et al.*[2] for an elastic half-space, and Neubauer[3] for a bounded beam. Goswami[4] first solved the fluid-solid curved surface problem in the presence of a Gaussian beam using the boundary element method. His method posed no restrictions on the shape of the surface, but required the use of a specialized wave with band-limiting properties, namely the Gaussian wave. The method developed here has no such restrictions.

The Model

An acoustic wave, generated in the fluid, is incident on the solid elastic medium as shown in Figure 1. On interaction, "scattered" waves are produced in the fluid and the solid. The total field (incident + scattered) is used as the primary variable in the formulation. This field has the disadvantage of not decaying far from the scatterer. As a result, the model cannot be truncated to a small neighborhood of the surface irregularity where most of the scattering effects are experienced. The technique developed here allows truncated models. This is achieved by splitting the total field into three components: incident, reflected, and scattered.

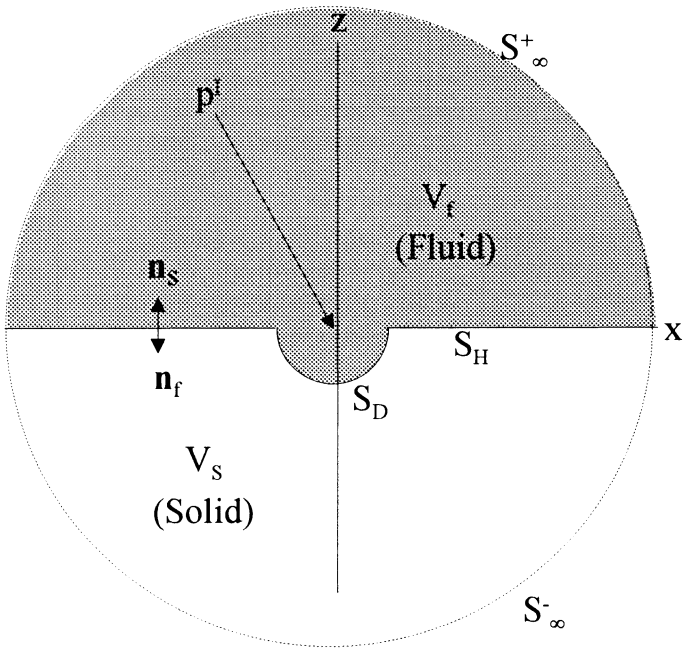

Figure 1: The fluid-solid interaction model

The total acoustic pressure p and its normal derivative $q = \nabla p \cdot \mathbf{n}$ in the fluid is decomposed into three parts,

$$p = p^I + p^R + p^s \tag{1}$$

$$q = q^I + q^R + q^s \tag{2}$$

where the scattered portions of the fields (p^S and q^S) are equal to zero in the absence of the scatterer (dimple). The incident and reflected portions correspond to the fields due to the flat part of the fluid-solid interface.

A similar decomposition of the total elastic field is made such that

$$\mathbf{u} = \mathbf{u}^t + \mathbf{u}^s \tag{3}$$

$$\mathbf{t} = \mathbf{t}^t + \mathbf{t}^s \tag{4}$$

where $\mathbf{u}^t$ is the transmitted displacement in the solid and $\mathbf{t}^S$ is the scattered traction in the solid due to the dimple on the interface. Hence the scattered fields diminish with increasing distance from the dimple. This property is used to truncate the model to a finite radius from the scatterer. The incident, transmitted, and reflected fields are numerically computed as presented in Ewing[5] and Shenoy[6].

At the fluid-solid interface S, the acoustic pressure p and the solid traction **t** are required to satisfy equilibrium and momentum balance conditions on the interface, such that

$$p(\mathbf{x})\mathbf{n}_f(\mathbf{x}) = -\mathbf{t}(\mathbf{x}) \qquad \mathbf{x} \in S \tag{5}$$

$$q(\mathbf{x}) = \rho_f \omega^2 \mathbf{u}(\mathbf{x}) \cdot \mathbf{n}_f(\mathbf{x}) \qquad \mathbf{x} \in S \tag{6}$$

where ρ_f is the fluid density, ω is the wave frequency, and **n** is the surface normal.

Boundary Element Formulation

The problem associated with each region is modeled using the respective full-space fundamental solution. As shown in Figure 1, the fluid domain V_f is bounded by S_∞^+, S_H, and S_D, and the solid domain V_S is bounded by S_∞^-, S_H, and S_D, where the subscripts H and D refer to the halfspace and dimple, respectively, and ∞ refers to the infinitely large outer boundary. The boundary S_H is further split into two parts, S_{HU} and S_{HM}, where S_{HU} is the unmodeled part of the interface and S_{HM} is the modeled part as shown in Figure 2.

Figure 2: The Interface model

The starting point is the acoustic representation integral,

$$p^s(\mathbf{x}) + \int_S \mathbf{G}(\mathbf{r})\, p^s(\mathbf{y})\, ds = \int_S \mathbf{F}(\mathbf{r})\, q^s(\mathbf{y})\, ds \qquad \mathbf{x} \in V_f,\ \mathbf{y} \in S \tag{7}$$

where $S = S_D + S_{HM} + S_{HU} + S_\infty^+$ is the boundary. This integral is written as

$$p_0^s + \int_{S_D+S_{HM}} \mathbf{G}p^s\, ds = \int_{S_D+S_{HM}} \mathbf{F}q^s\, ds + \int_{S_{HU}} \left(\mathbf{F}q^s - \mathbf{G}p^s\right) ds + \int_{S_\infty^+} \left(\mathbf{F}q^s - \mathbf{G}p^s\right) ds \tag{8}$$

where the integral on S_∞^+ is zero due to the Sommerfeld radiation conditions, and the integral on S_{HU} is zero since the scattered fields are assumed to be zero on S_{HU}.

The acoustic BIE is derived, using the static Green's functions to regularize Equation (8), as

$$\begin{aligned} &p^I + p_0^s\left[\frac{1}{2} - \int_{S_1} \mathbf{G}^S ds\right] + \int_{S_1} \mathbf{G}^D p^s ds + \int_{S_0} \left(\mathbf{G}^D - \mathbf{G}^S\right) p^s ds + \int_{S_0} \mathbf{G}^S \left(p^s - p_0^s\right) ds \\ &\quad = p^I + \int_S \mathbf{F}^D q^s ds \end{aligned} \tag{9}$$

The elastodynamic BIE is similarly obtained as

$$\begin{aligned} &\mathbf{u}^I + \mathbf{u}_0^s\left[\frac{1}{2}\mathbf{I} - \int_{S_1} \mathbf{T}^S ds\right] + \int_{S_1} \mathbf{T}^D \mathbf{u}^s ds + \int_{S_0} \left(\mathbf{T}^D - \mathbf{T}^S\right) \mathbf{u}^s ds + \int_{S_0} \mathbf{T}^S \left(\mathbf{u}^s - \mathbf{u}_0^s\right) ds \\ &\quad = \mathbf{u}^I + \int_S \mathbf{U}^D \mathbf{t}^s ds \end{aligned} \tag{10}$$

where the superscripts S and D on the fundamental solutions indicate static and dynamic, respectively.

Multi-Region Boundary Element Method

To solve equations (9) and (10) efficiently, the usual boundary element method was modified to solve multi-region problems. The equations are discretized (after removing the incident wave information on both sides), to obtain

$$[\mathbf{A}]\{p^s\} = [\mathbf{B}]\{q^s\} \tag{11}$$

$$[\mathbf{C}]\{\mathbf{u}^s\} = [\mathbf{D}]\{\mathbf{t}^s\} \tag{12}$$

These equations are modified to replace the scattered field variables with their total field counterparts. Equation (11) is written as

$$\{p^s\} = \mathbf{A}^{-1}\mathbf{B}\{q^s\} \tag{13}$$

The total incident fields can be written as

$$\begin{aligned} p^I &= p^{\text{incident}} + p^{\text{reflected}} \\ \mathbf{u}^I &= \mathbf{u}^{\text{transmitted}} \end{aligned} \tag{14}$$

Similar expressions may be written for q and **t**. Adding p^I to both sides of equation (13) to obtain

$$\{p^t\} = \mathbf{A}^{-1}\mathbf{B}\left(\{q^t\} - \{q^I\}\right) + \{p^I\} \tag{15}$$

where the superscript t indicates the total field. Using the matrix **N** given by

$$\mathbf{N} = \begin{bmatrix} n_1^1 & n_2^1 & n_3^1 & 0 & \dots & \dots & \dots & \dots & \dots & 0 \\ 0 & 0 & 0 & n_1^2 & n_2^2 & n_3^2 & 0 & \dots & \dots & \vdots \\ \vdots & \ddots & \ddots & \ddots & \ddots & \ddots & \ddots & \dots & \dots & \vdots \\ \vdots & \ddots & \ddots & \ddots & \ddots & \ddots & \ddots & \dots & \dots & 0 \\ 0 & \dots & \dots & \dots & \dots & \dots & 0 & n_1^N & n_2^N & n_3^N \end{bmatrix} \tag{16}$$

containing the nodal normals, and its transpose $\mathbf{N}^T$, equation (15) is written as

$$\mathbf{N}^T\{p^t\} = \mathbf{N}^T\mathbf{A}^{-1}\mathbf{B}\left(\{q^t\} - \{q^I\}\right) + \mathbf{N}^T\{p^I\} \tag{17}$$

Using the interface conditions (5) and (6), the fluid equation is written in the traction/displacement form as

$$\{\mathbf{t}^t\}^F = \left(-\rho_f\omega^2\right)\mathbf{N}^T\mathbf{A}^{-1}\mathbf{B}\mathbf{N}\{\mathbf{u}^t\} + \mathbf{N}^T\mathbf{A}^{-1}\mathbf{B}\{q^I\} - \mathbf{N}^T\{p^I\} \tag{18}$$

Similarly, the solid equation is written as

$$\{\mathbf{t}^t\}^S = \mathbf{D}^{-1}\mathbf{C}\{\mathbf{u}^t\} - \mathbf{D}^{-1}\mathbf{C}\{\mathbf{u}^I\} + \{\mathbf{t}^I\} \tag{19}$$

Since,

$$\{\mathbf{t}^t\}^F + \{\mathbf{t}^t\}^S = \{0\} \tag{20}$$

on the interface, the combined system equation is

$$\begin{aligned} &\left[\mathbf{D}^{-1}\mathbf{C} - \rho_f\omega^2\mathbf{N}^T\mathbf{A}^{-1}\mathbf{B}\mathbf{N}\right]\{\mathbf{u}^t\} \\ &\quad = -\mathbf{N}^T\mathbf{A}^{-1}\mathbf{B}\{q^I\} + \mathbf{N}^T\{p^I\} + \mathbf{D}^{-1}\mathbf{C}\{\mathbf{u}^I\} - \{\mathbf{t}^I\} \end{aligned} \tag{21}$$

The right hand side of equation (21) contains the vector involving the incident field quantities. Therefore, any type of wave may be used provided these incident field quantities for the wave are available.

The only unknowns in equation (21) are the surface displacements. On obtaining these displacements, the tractions are obtained using equation (19). The fluid fields p and q may then be calculated using the interface conditions.

Results

A boundary element mesh was constructed as shown in Figure 3. An aluminum solid, immersed in water, contained the water-filled dimple. A circular area (radius = 4*dimple radius) on the interface was discretized. A plane compressional wave was generated within the fluid.

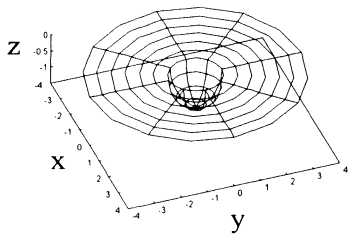

ω = 0.894MHz
Radius of Dimple = 1.0
k_f = 6.0
k_L = 1.4010
k_T = 2.8656
Nodes = 241
Elements = 80

Figure 3: BEM model of a fluid-filled dimple on the fluid-solid interface

The scattered pressure was computed on the boundary, in the x-z plane, and plotted (Figure 4) for various incidence angles in the fluid. As expected, the maximum amplitude was on and around the z-axis. This peak shifted to the right of the z-axis as the incidence angle (measured counter-clockwise from the z-axis) was increased. The scattered pressure amplitude on the flat surface and the backscattered pressure decreased as the distance from the dimple increased. Solution convergence was verified using various mesh sizes and increasing the discretized area. Reciprocity checks were also performed on the computer program.

Since analytical and experimental results were unavailable for a problem of this complexity, the program was checked using results to problems, in the literature, where a solution was available. A plane compressional wave was generated in the solid along the z-axis in the x-z plane. In the absence of the fluid, the results (Figure 5) presented in Sanchéz-Sesma[7] compared very well with those computed using our program.

Two other problems were solved using the same wave - a fluid filled dimple and an air filled dimple, and the results presented in Figure 6. As expected, the traction-free surface exhibited the strongest displacements. The fluid-filled case and the air bubble case (using a pressure free fluid-bubble interface and a traction-free bubble-solid interface) had lower surface displacements due to the fact that some of the energy was dissipated in the fluid.

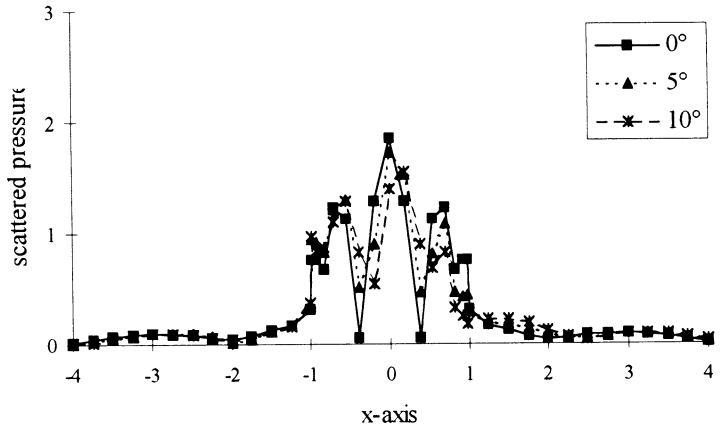

Figure 4: Scattered boundary pressure amplitude

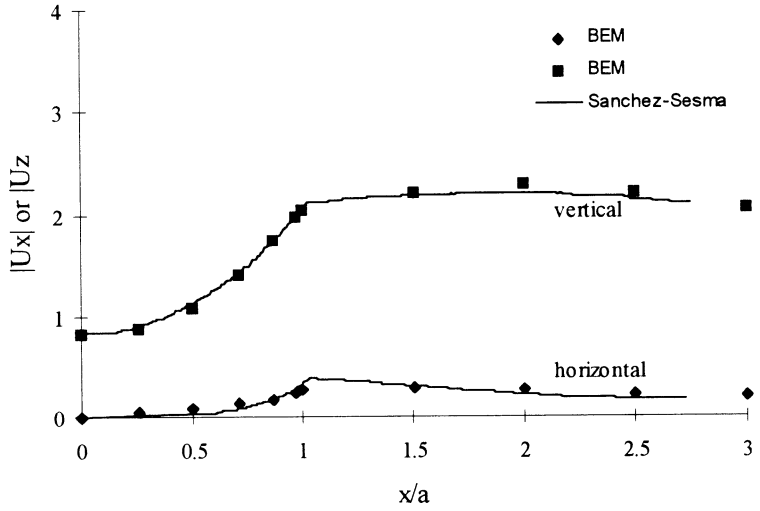

Figure 5: Displacement amplitudes in the x-z plane due to scattering by a dimple

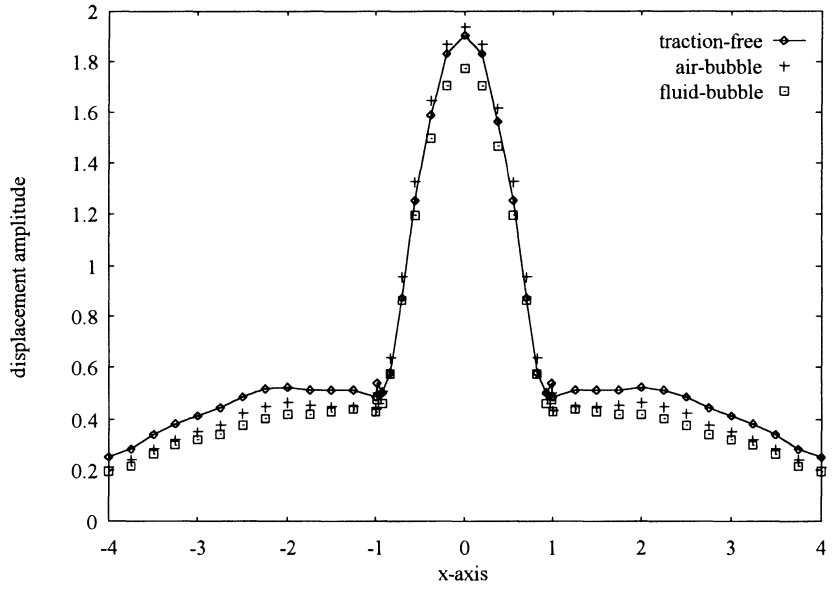

Figure 6: Scattered displacements on the solid surface

References

1. Luco, J. E., & Apsel, R. J., On the Green's Functions for a Layered Half-space. Part I, *Bull. Seism. Soc. Am.*, **73**, 909-929.
2. Rizzo, F. J., Shippy D. J., & Rezayat M., A Boundary Integral Equation Method for Time-Harmonic Radiation and Scattering in an Elastic Half-Space, in Advanced Topics in Boundary Element Analysis, (ed T. A. Cruse, A. B. Pifko and H. Armen), pp. 83-90, *ASME Winter Annual Meeting*, Miami Beach, Florida, Nov. 1985, ASME, New York, 1985.
3. Neubauer, W. G., Ultrasonic Reflection of a Bounded Beam at Rayleigh and Critical Angles for a Plane Liquid-Solid Interface, *J. Appl. Physics*, 1973, **44**, 48-55.
4. Goswami, P. *Application of the boundary element method to coupled fluid-structure interaction problems*, Ph.D. Thesis, Iowa State University, Ames, Iowa, 1991.
5. Ewing, W.M., Jardetzky W.S., & Press, F. *Elastic Waves in Layered Media,* McGraw-Hill, New York, 1957.
6. Shenoy, S. *Boundary element solutions to wave scattering by surface anomalies on a fluid-solid interface*, Ph.D. Thesis, Iowa State University, Ames, Iowa, 1994.
7. Sanchéz-Sesma, F.J. Diffraction of elastic waves by three-dimensional surface irregularities, *Bull. Seism. Soc. Am.*, **73**, 1621-1636.